Composite Structures 134 (2015) 10–17

Contents lists available at ScienceDirect

Composite Structures

journal homepage: www.elsevier.com/locate/compstruct

Investigation for the bending modes of a semi-circular pyramidal kagome sandwich structure and the bending load calculation

June-Sun Hwang [a], Tae-Gyun Choi [b], Min-Young Lyu [b], Dong-Yol Yang [a,*]

[a] School of Mechanical Aerospace & Systems Engineering, KAIST, 291 Daehak-ro, Yuseong-gu, Daejeon, Republic of Korea
[b] Department of Product Design Manufacturing Engineering, Graduate School of Seoul National University of Science and Technology, 232 Gongneung-ro, Nowon-gu, Seoul 139-743, Republic of Korea

ARTICLE INFO

Article history:
Available online 7 August 2015

Keywords:
Lattice
Pyramidal kagome structure
Shear modulus
Specific bending stiffness

ABSTRACT

Lattice-based sandwich structures are being widely investigated to meet increasing demands for lightweight components. In the recent research works, lattice-based open cell structures have exhibited higher specific strength compared to closed cell structures, such as a honeycomb structure. Generally, a kagome structure is more effective than other lattice structures for compression and bending. In this work, cross-sections of the strut of pyramidal kagome (PK) structure are developed to strengthen the sandwich structure. A PK structure based on a semi-circular cross-section (SCC) was applied to the bending load calculation. The bending deformation modes of the SCC-based PK sandwich structure were investigated. The bending load was calculated when the PK sandwich structure was bent as stable shear mode and the equation could express the non-linear elastic characteristics during the bending process by applying the effective shear modulus of inner PK cores. The calculated bending load–deflection curve was compared with the bending load–deflection curve obtained by FEM. The tendency of the calculated bending load–deflection curve was similar to the FEM result.

1. Introduction

Sandwich structures that are composed of face sheets and a designed inner core are very effective in terms of specific strength [1,2]. Truss based structures, which are referred to as open cell structures, have some advantages over closed cell structures, and for this reason open cell structures are considered to be desirable alternatives to closed cell structures [3–5]. An open cell structure subject to in-plane shear load has more strength than a honeycomb structure, and the open cell structure can easily include additional functional properties by filling with a heat insulation material [6]. The other advantage of the open cell structure is its high specific strength compared to the closed cell structure [7]. The fabrication methods and mechanical characteristics of open cell truss cores have been investigated for an octahedral truss [8], pyramidal truss [9,10], and tetrahedral truss [11,12], kagome structure [13–15], and so on. The above studies on truss structures demonstrated that the kagome structure has superb mechanical properties. Generally, the kagome structure has been fabricated by a weaving method [16], laser melting method [17], or investment casting method [18]. However, the fabrication time is typically long because of the complicated process, and production cost is also expensive.

Most of the truss structures in these studies were based on struts with rectangular cross-section [19,20] or round wire struts [21]. Recently, sandwich structures based on metal tubes such as the tube-woven kagome structure [22] and hollow truss pyramidal lattice [23] have been introduced. There was also an attempt to make a hollow composite truss structure using CFRP [24]. Even though there have been a few studies on the cross-sectional effect of truss core structures, research works on fabrication processes employing hollow struts with triangular or square cross-sections [25] is subject to further investigation.

In addition, the stress analysis of the composite sandwich structure which has complicated cross-sections became more difficult because of its huge number of elements for the complicated cross-sectional area. There were attempts for analysis of composite sandwich structure by the homogenization method [26], calculating the elastic load and the critical fracture load of sandwich structure [27]. However, there was no attempt to calculate the bending load of truss sandwich structure including the non-linear deformation of inner cores.

* Corresponding author. Tel.: +82 42 350 3214; fax: +82 42 350 5214.
E-mail address: dyyang@kaist.ac.kr (D.-Y. Yang).

http://dx.doi.org/10.1016/j.compstruct.2015.08.017
0263-8223/

In this paper, the method for bending load calculation for the composite sandwich structure has been developed. The bending deformation modes were categorized into three types such as stable shear, local compression, and face wrinkling according to gap distance between two neighboring inner cores and a ratio of bending stiffness of the face sheet to the shear stiffness of inner cores. The bending load was calculated only in the case that the specimen was bent as the stable shear mode. The shear deformation of inner cores was approximated and the shear modulus of inner cores was calculated according to its shear deformation. The shear modulus value was obtained from the pure shear load–displacement curve of the unit core structure. The bending load of the composite sandwich structure was calculated by using the shear moduli of cores. The bending load calculation was conducted with a pyramidal kagome (PK) structure which had the semi-circular cross-section.

2. PK core structure design and materials

The manufacturing process of the polymer PK structure was developed in the previous research [28]. The PK structure was fabricated by the injection molding and adhesive bonding process. The flat mesh was fabricated by the injection molding process as shown in Fig. 1(a). The pyramidal structures that are shown in Fig. 1(b) were formed from the flat mesh. Two pyramidal structures were welded face-to-face by ultra-sonic wave welding device as shown in Fig. 1(c). The inner PK structure was made of polypropylene and the PK structure was bonded adhesively with the GFRP face sheets as shown in Fig. 1(d).

2.1. Cross-sectional design for core strut

The cross-section of the PK structure was a flat rectangular shape in the previous research [28]. The rectangular strut was weak in terms of sustaining the bending load and the structure is vulnerable to buckling. The PK structure could be strengthened by changing the cross-sectional shape of the PK structure because the critical buckling load is proportional to Young's modulus and the geometrical moment of inertia of the strut. Even though the cross-section areas are same, the moment of inertia can be greatly increased depending on the cross-sectional shape. A tubular and a semi-circular cross-sections were considered as improved alternatives to the conventional PK structure based on flat rectangular cross-sections. The designed cross-sections of the strut are shown in Fig. 2. The cross-sectional areas were same as 0.6 mm^2 while the moment of inertia of the tubular cross-section was 4.4 times greater than that of rectangular shape. The mechanical strength including the bending stiffness and strength could be improved by changing the cross-sectional shape from a flat rectangular shape to a tubular or semi-circular shape.

The investigation of bending deformation modes was made with the SCC-based PK sandwich structure because the fabrication process of SCC-based PK structure was easier than the tubular shape. Moreover, the difference of geometrical moment of inertia between the semi-circular cross-section and round tubular cross-section was small. The SCC-based PK structure was designed as shown in Fig. 3. The strut angle, θ, was 45° which was the optimum angle from the previous research [28]. The height of the core, c, was 3.6 mm. The thickness of the core, t_c, was 0.4 mm. The width of the core, w, and unit length of the core, l, were 1.36 mm and 4.18 mm, respectively.

2.2. Analysis modeling for the bending deformation mode

Generally, the failure of the sandwich structure occurs as face yielding, face wrinkling, core yielding, core buckling, and face indentation [27]. However, composite sandwich structures composed of strong face sheets do not easily fail by face yielding and face indentation. Therefore, the failure modes of face wrinkling, core buckling, and local compression were investigated for the composite sandwich structure. The three failure modes of sandwich were expressed by the bending deformation mode in this work. An adhesive failure between the core and face sheets was not considered because the adhesive failure did not occur in the similar bending condition [28].

The bending deformation of a sandwich structure can be affected by design parameters such as a gap distance and a flexural rigidity of the face sheet. The gap distance means the distance between the PK structures. From the reason, the major parameter for the deformation mode was the ratio of bending stiffness of the face sheet to shear stiffness of the inner cores and the gap distance between the inner cores. The analysis for the bending deformation mode was conducted with five different stiffness ratios as shown in Table 1. The gap distance was varied from 0 mm to 7.5 mm with 0.15 mm of increments.

The bending analysis was conducted by the commercial finite element analysis software (ABAQUS, Dassault systems, France). The bending specimen was designed as a 1/2 scale model and a symmetric boundary condition was applied. The bending specimen model is shown in Fig. 4. The thickness of the face sheet, t_f, was 0.6 mm and the core structure was designed as the SCC-based PK structure. The length of the face sheet, L_f, was 120 mm. The width, b, of the sandwich structure was 4.2 mm. The diameters of the rolls were 4 mm and the span length between bottom rolls, L, was 75 mm. The bending deflection was set to be 7.0 mm.

The material properties were examined by material tests and applied to the analysis. Young's modulus of polypropylene, Poisson's ratio, and yield strength of polypropylene were 1222 MPa, 0.35, 15 MPa, respectively. The true plastic stress vs. true plastic strain curve was calculated and applied to the analysis. Young's modulus of the GFRP and Poisson's ratio material was

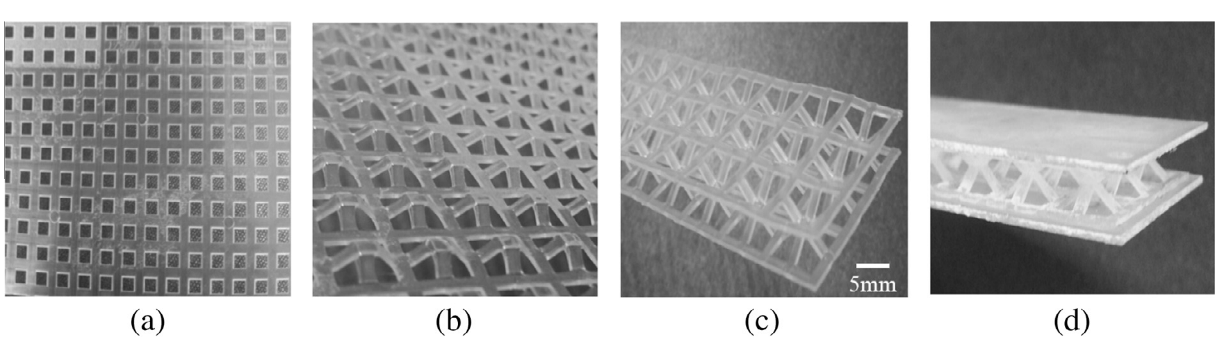

Fig. 1. Fabrication of the pyramidal kagome structure: (a) flat mesh; (b) pyramidal core; (c) pyramidal kagome structure; (d) pyramidal kagome sandwich structure.

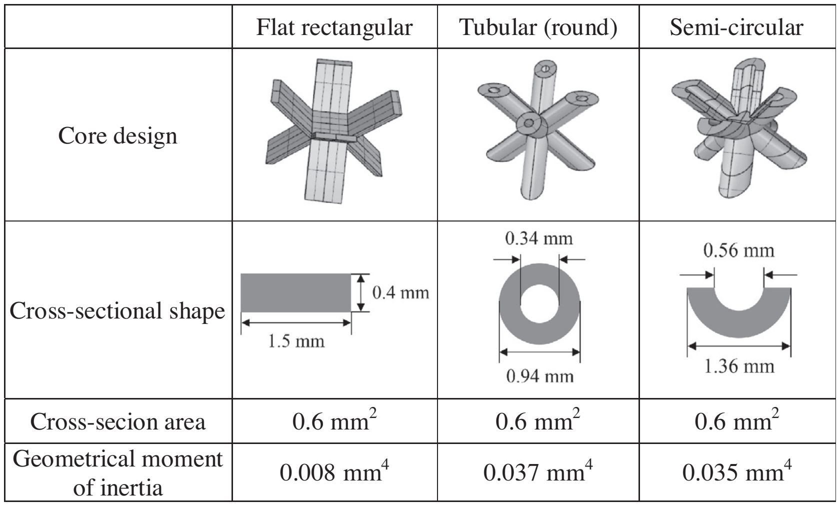

Fig. 2. Geometrical moment of inertia according to different cross-sectional shapes.

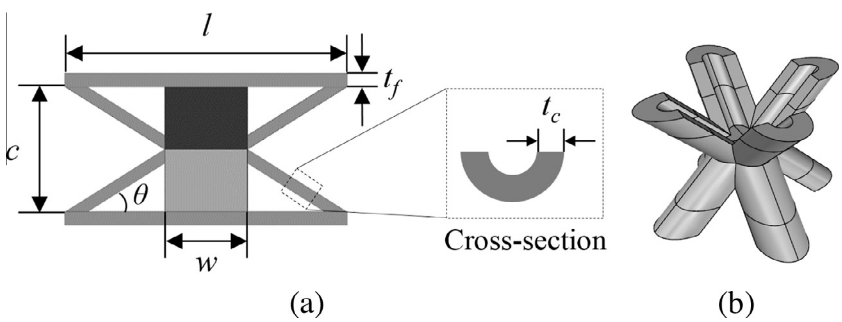

Fig. 3. Designed SCC-based PK structure: (a) dimensions of SCC-based PK structure; (b) perspective view of SCC-based PK structure.

Table 1
Parameters for bending mode analysis.

	Young's modulus (GPa)	Thickness of face sheet, t_f (mm)	Flexural rigidity of face sheet, D_f (N mm^2)	Shear rigidity of core, AG_c (N/mm)	D_f/AG_c, (mm^3)
Case 1	30	0.6	666,792	150	4445
Case 2	15	0.6	333,396	100	3334
Case 3	15	0.5	264,758	100	2648
Case 4	30	0.3	287,469	150	1916
Case 5	15	0.3	143,734	150	958

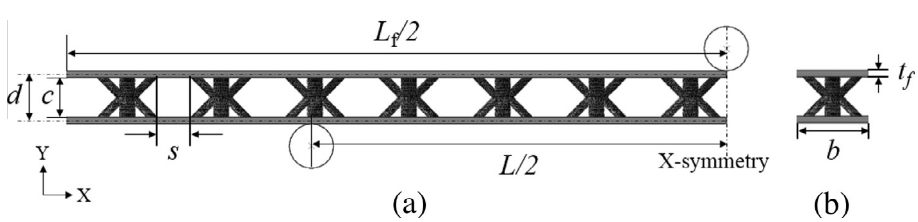

Fig. 4. Model of the three-point bending analysis: (a) front view; (b) side view.

30 GPa, 0.34, respectively. The number of elements for the SCC-based PK structure was 18,672.

3. Results of bending deformation mode

The bending deformation mode could be changed according to the ratio of the bending stiffness of the face sheet to the shear stiffness of the inner core and the gap distance between the PK structures. The major bending deformation came about as the stable shear mode, local compression mode, and face sheet wrinkling mode as shown in Fig. 5.

When the bending stiffness of the face sheet and the shear stiffness of the inner core were balanced, the sandwich structure was bent with stable shear mode as shown in Fig. 5(a). The local compression mode occurred when the shear stiffness of the core was higher than the bending stiffness of the face sheet and the gap

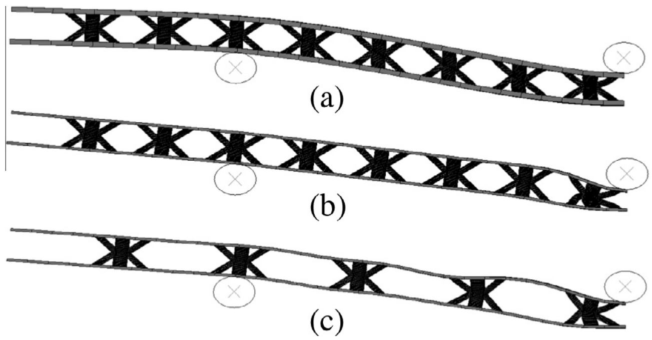

Fig. 5. Major bending deformation: (a) stable shear mode with case 2 ($s/L = 0.02$); (b) compression mode with case 4 ($s/L = 0.02$); (c) face sheet winkling mode with case 5 ($s/L = 0.1$).

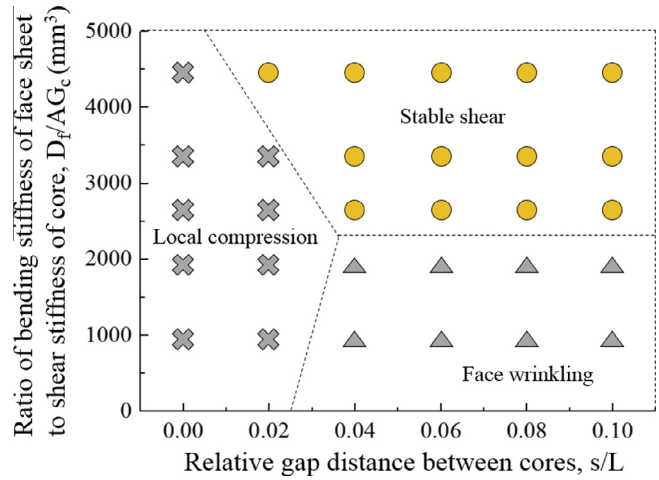

Fig. 7. Bending deformation window for composite sandwich structure.

distance between the PK structures was small enough. The local compression mode was not stable and the excessive inner cores made the sandwich structure heavier. Face sheet wrinkling occurred when the gap distance between the PK structures became large.

The load–deflection curve of the specimens is shown in Fig. 6. When the specimen was bent with the stable shear mode, the bending load–deflection curve became stable. The bending load increased stably without decrease. However, when the local compression mode occurred, the bending load decreased after bending deflection of 3 mm because the local area of specimen was compressed excessively. In case of the specimen shown in Fig. 5(c), the specific bending stiffness was 75% lower than the specific bending stiffness of the specimen shown in Fig. 5(a) because of its low stiffness ratio. The stable shear mode was desirable from the viewpoint of specific strength among the three deformation modes.

Three bending deformation mode were classified into local compression, stable shear, and face wrinkling on the bending deformation window as shown in Fig. 7. Each symbol in the bending deformation window means that the analysis was conducted with the coordinate value of the stiffness ratio and the relative gap distance.

The specimens were bent with local compression mode when the relative gap distance became less than 0.02 except in case 1. The local compression mode was defined when the specimen was compressed more than 20% in the center area. The stable shear mode and face wrinkling mode occurred when the relative gap distance was above 0.04. When the stiffness ratio was higher than 2648 mm^3, the stable shear mode was dominant, and when the ratio was lower than 1916 mm^3, the face wrinkling mode appeared.

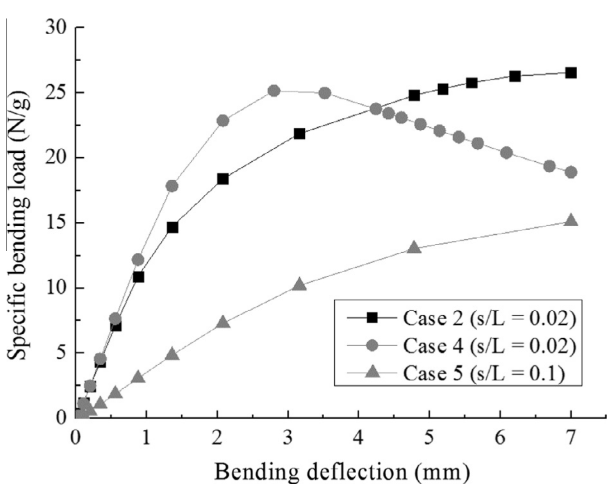

Fig. 6. Specific bending load–deflection curves according to bending mode.

When the specimen was bent as stable shear mode, the bending load could be calculated by considering the bending load of the face sheets and the shear load of the inner core. Actually, the specimen was bent with complex loading, however the complex loads could be assumed as combination of two major loads, i.e. bending load for face sheet and the longitudinal shear load for the inner core. To calculate the longitudinal shear load of the core, the shear modulus of the inner core was needed and the shear modulus could be calculated by considering the shear deformation curve of the inner core. The shear deformations of the inner core were measured from the analysis results, and the obtained shear deformation curves are shown in Figs. 8 and 9.

The effect of the stiffness ratio between the face sheet and the core with the same gap distance is shown in Fig. 8. The shear deformation curve of the inner cores was not much affected by the stiffness ratio because the deformation curves of case 1 and case 2 were very similar even when the stiffness ratio of the specimen increased by 33.4%. However, the shear deformation curve was much affected by the gap distance as shown in Fig. 9. The shear deformation considerably increased from zero to 40 mm according to the gap distance increased. When the longitudinal distance was 20 mm in the Fig. 9(a), the shear deformation increased by 51% when the relative gap distance increased from 0.04 to 0.1. The shear deformation curve of the inner cores seemed to be mainly affected not by the stiffness ratio but by the gap distance between the cores because the shear deformation was mainly changed by the relative gap distance. The shear deformation curve could be approximated if the gap distance and stiffness ratio were fixed and used to calculate the shear modulus of the inner core.

4. Bending load prediction model

The bending analysis of various cross-sections of PK sandwich structures takes a long time for element generation and the numerical bending analysis because there are more than 200,000 elements for the PK sandwich structure. The calculation of the bending load of the foam core sandwich was formulated by Allen [29] as equation (1), where δ is the total bending deflection, δ_b and δ_s is the bending deflection which was generated by the bending deformation of the sandwich structure and the shear deformation of the sandwich structure, respectively. The L_s is the span

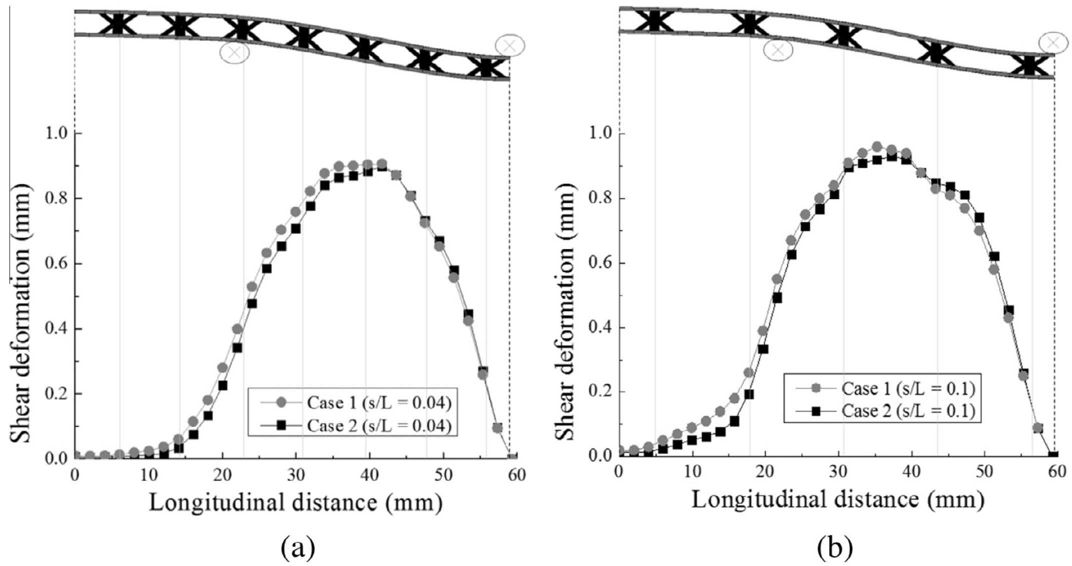

Fig. 8. Comparison of shear deformation of inner cores according to face sheet vs. inner core stiffness ratio: (a) $s/L = 0.04$; (b) $s/L = 0.1$.

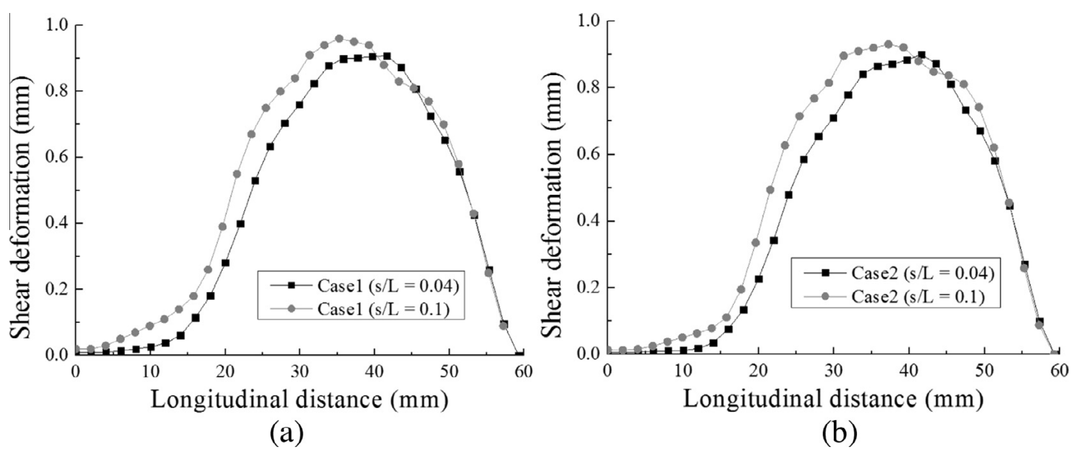

Fig. 9. Comparison of shear deformation of inner cores according to gap distance: (a) case 1 ($D_f/AG_c = 4445$); (b) case 2 ($D_f/AG_c = 3333$).

Table 2
Dimensions and material property of the SCC-based PK sandwich structure.

Core thickness, c (mm)	3.6
Face sheet thickness, t_f (mm)	0.6
Width of sandwich structure, b (mm)	4.2
Distance between the center of face sheets, d (mm)	4.2
Span length, L (mm)	75
Length of face sheet, L_f (mm)	120
Elastic modulus of face sheet, E_f (GPa)	30
Gap distance, s (mm)	2.5

length between two lower rolls, E_f and G_c are the elastic modulus of the face sheet and the shear modulus of the inner core, respectively, c is the height of the inner core, b is the width of the sandwich structure, t_f is the thickness of the face sheet, and d is the distance between the center lines of two face sheets. The bending load calculation was conducted with the SCC-based PK sandwich structure and the dimensions are indicated in Fig. 4 and Table 2.

$$\delta = \delta_b + \delta_s = \frac{PL_s^3}{48E_f\frac{bt_f d^2}{2}} + \frac{PL_s}{4\frac{bd^2}{c}G_C} \quad (1)$$

The bending load could be calculated with Eq. (1). However, the non-linear characteristic of the inner core structure was not considered in the equation. In some research works, the bending load was obtained by calculating the elastic area and non-linear area, respectively. In the separated calculation, Eq. (1) was applied to the calculation of elastic bending load and the core shear failure load or the face indentation load was applied to a non-linear load [27,30]. Even though non-linear loading could be described in calculating the bending load, the bending load shows considerable error compared with the experimental results. In this study, the non-linear bending load of the sandwich structure was calculated by applying the effective shear modulus of the core to calculate more accurate bending load.

4.1. Calculation of effective shear modulus of truss cores

The bending load calculation for the face sheet bending is relatively simple because the face sheet is deformed elastically. However, the bending load calculation for the inner core is more complex because the shear load was affected by critical buckling load or shear stiffness of the inner core. The non-linear characteristic was obtained by considering the shear deformation of inner core.

In this work, bending load was calculated by considering the shear modulus of sixteen PK cores. The shear modulus was calculated from the shear deformation of the PK structures. The non-

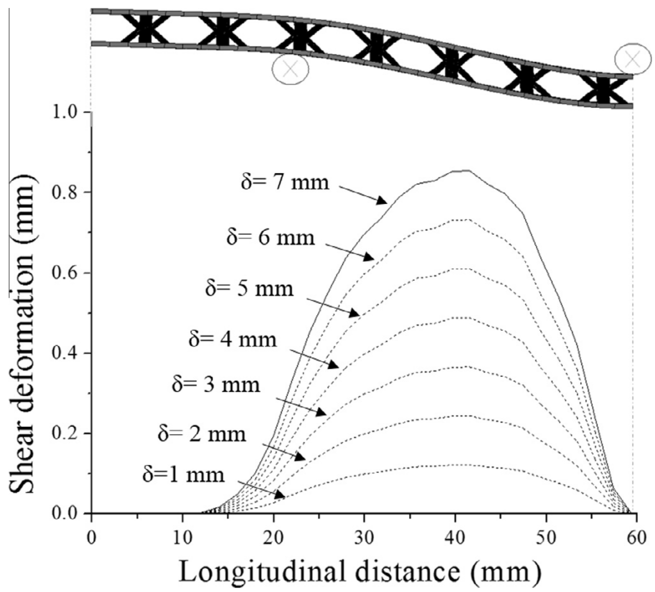

Fig. 10. Shear deformation of inner core according to longitudinal direction.

linear characteristics of the PK structures including buckling or yielding of cores were included in the shear deformations of cores and the non-linear bending deformation could be expressed. The shear deformations of the inner cores during the bending process are shown in Fig. 10. The distribution of shear deformation at the deflection of 7.0 mm was shown as approximated by using the bending deformation window and its shear deformation curves. The other curves for shear deformation distribution were proportionally approximated based on the shear deformation curve when the deflection was 7.0 mm. The bending increment was set to 0.1 mm from 0 to 6.9 mm.

When the shear deformation of the PK structure was determined from the shear deformation curve, the middle coordinates of each PK structure was defined as representative shear deformation of each PK structure. The representative shear deformation value was used because the shear deformation was varying even in the unit PK structure according to the location in the longitudinal direction. The shear modulus of PK structures was calculated by using the representative shear deformation value. The representative shear deformation of each PK core was expressed as the shear strain, γ, and the shear moduli of eight PK structures were calculated by the γ value in each bending increment. The shear modulus of each PK structures was calculated based on the pure shear stress–strain curve of unit PK structure. The pure shear stress–strain curve of the unit PK structure is shown in Fig. 11 (b). The shear stress–strain curve was expressed as an exponential function, as shown in Eq. (2), and the derivative of Eq. (2) is shown in Eq. (3). The shear modulus of each PK structure was calculated by substituting the representative shear strain, γ, to Eq. (3)

$$\tau(\gamma) = -0.83921\, e^{\left(-\frac{\gamma}{0.21838}\right)} - 2.00654\, e^{\left(-\frac{\gamma}{0.01954}\right)} \tag{2}$$

$$\tau'(\gamma) = \frac{0.83921}{0.21838}\, e^{\left(-\frac{\gamma}{0.21838}\right)} + \frac{2.00654}{0.01954}\, e^{\left(-\frac{\gamma}{0.01954}\right)} \tag{3}$$

The shear moduli of eight PK structures were calculated from zero to 7.0 mm in deflection with the increment of 0.1 mm and the shear moduli of eight PK structures were averaged in each bending increment as the effective shear modulus of the inner core. The effective shear modulus distribution according to the bending deflection is shown in Fig. 12. The effective shear modulus decreased depending on the deflection because elastic buckling was generated in the PK sandwich structures according to the bending deflection.

4.2. Bending load calculation

The flexural rigidity of the sandwich structure is generally expressed by Eq. (4). The first term and the third term were neglected because the effect of flexural rigidity of the faces about their own separate axis and inner core was very small. The second term was used for calculation of the flexural rigidity.

$$D = E_f \frac{bt_f^3}{6} + E_f \frac{bt_f d^2}{2} + E_c \frac{bc^3}{12} \tag{4}$$

When the deflection of shear deformation of the sandwich structure was calculated, shear deformation of the face sheet was neglected because the face sheet is too thin to be deformed in cross-sectional shear. The bending load was calculated by Eq. (1) and the effective shear modulus of eight PK structures was applied to the equation. The small compressive deformation of the PK structure, which was located at the center area, was also considered based on the compressive deformation–deflection curve shown in Fig. 13. The additional compression due to the compressive deformation at the center area was added to the left term of Eq. (1) as the additional deflection.

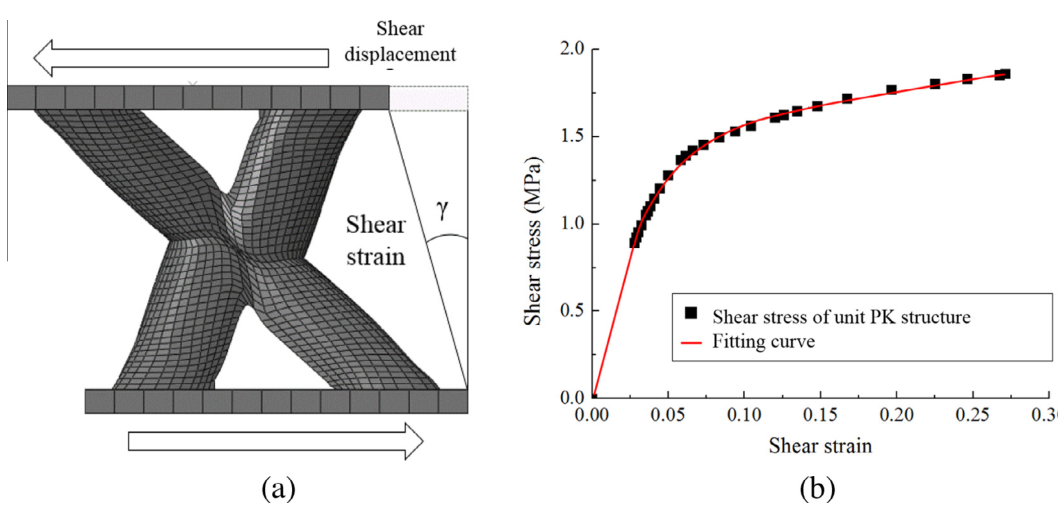

Fig. 11. Shear stress–strain relation of unit PK structure: (a) shear analysis model; (b) shear stress–strain curve.

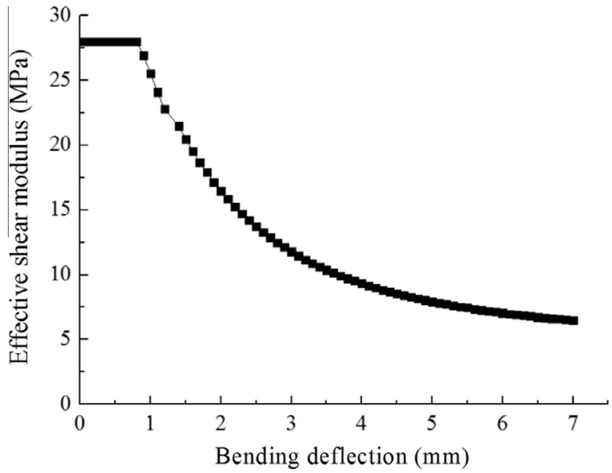

Fig. 12. Variation of effective shear modulus for eight PK structures according to bending deflection.

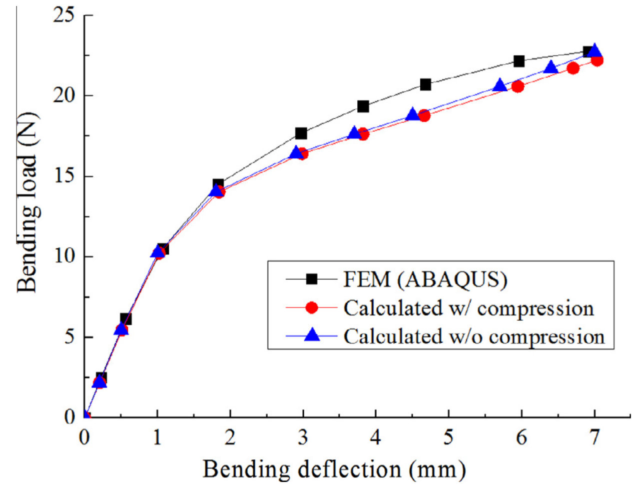

Fig. 14. Comparison of bending load of SCC-based PK sandwich structure between calculation and FEM.

4.3. Results and discussion

The calculated bending load during three-point bending is shown in Fig. 14 and the results were compared with the FEM result which was designed with the same parameters of bending load calculation. The bending load–deflection distribution was very similar to the computational results of the commercial FEM software which takes more than 10 times the computing time for the bending analysis compared with the load calculation. In the calculated bending load–deflection curve, the initial bending stiffness was exactly same as the FEM software. The maximum difference gap between the calculated value and FEM software was 9.0%.

Even though there were some errors in the bending load calculation, the non-linear characteristics during bending of the sandwich structure could be expressed by applying the effective shear modulus of the inner core. When compressive deformation was applied, the bending load curve was more accurate in the view point of bending load tendency. However, compressive deformation could be neglected because the deformation amount by compressive in the stable shear specimen was very small. If bending deflection increased, compressive deformation could become more significant.

Error may have occurred when the effective shear modulus was calculated. Firstly, the shear modulus of each eight PK structure was calculated based on the pure shear analysis results; however, PK structures actually take a complex load of shear and compression load. The shear modulus of each PK structure will be higher if the shear analysis is conducted with compression deformation and the bending load calculation could be more accurate. Secondly, error could occur when the shear deformation of each PK structure was represented as one value in the PK structure. The shear deformation of PK structure could be different following longitudinal direction even in one PK structure, however the shear deformation at the center point of each PK structure was used as the representative shear deformation of each PK structures and it can make the error. However, the bending load was calculated in a few minute with the error of 9% while the FEM software takes more than four hours. The bending mode window and the bending load calculation method could be helpful to design the composite sandwich structure and to understand the bending load–deflection tendency.

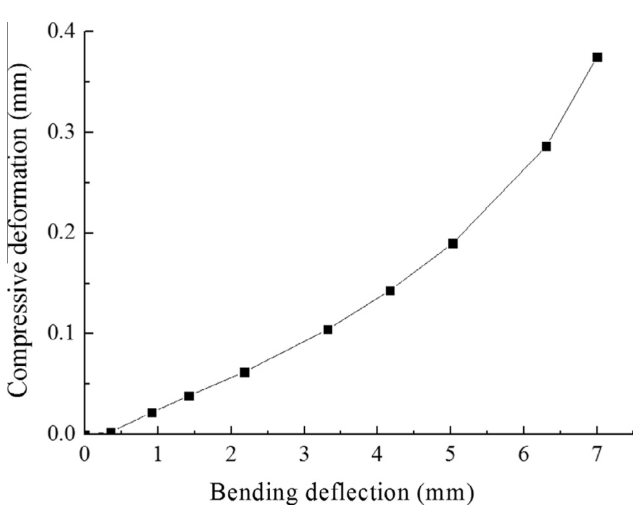

Fig. 13. Compressive deformation of a PK sandwich structure at the center.

5. Conclusion

The concept of bending load calculation of composite sandwich structure was suggested in this work. The semi-circular cross-section was applied and the geometrical moment of inertia increased 4.3 times as compared with rectangular cross-section. The bending deformation modes of the composite sandwich structure was investigated according to the ratio of bending stiffness of the face sheet to the shear stiffness of inner cores and relative gap distance between PK structures. Among the possible modes, i.e. the stable shear mode, local compression mode, and face wrinkling mode, the specimen bent with stable shear mode was considered as the best bending mode from the viewpoint of bending load distribution and weight optimization. The shear modulus of PK structures was calculated from the shear deformation of inner cores and the bending load of sandwich structure was calculated by using the effective shear modulus of PK structures. Even though there are some errors, the non-linear characteristic during the bending process was demonstrated in the bending load–deflection curve and the bending load tendency was very similar to the analysis result that was conducted by the FEM software. The bending load was calculated in a few minutes with the maximum error of 9% while the FEM software takes more than four hours. The bending mode window and its shear deformation curve are found to be useful for the designing of the composite sandwich structure.

References

[1] Xiong J, Ma L, Stocchi A, Yang JS, Wu LZ, Pan SD. Bending response of carbon fiber composite sandwich beams with three dimensional honeycomb cores. Compos Struct 2014;108:234–42.
[2] Du YC, Yan N, Kortschot MT. An experimental study of creep behavior of lightweight natural fiber-reinforced polymer composite/honeycomb core sandwich panels. Compos Struct 2013;106:160–6.
[3] Lu TJ, Valdevit L, Evans AG. Active cooling by metallic sandwich structures with periodic cores. Prog Mater Sci 2005;50(7):789–815.
[4] Xiong J, Ghosh R, Ma L, Ebrahimi H, Hamouda AMS, Vaziri A, et al. Bending behavior of lightweight sandwich-walled shells with pyramidal truss cores. Compos Struct 2014;116:793–804.
[5] Kohrs T, Petersson BAT. Wave propagation in light weight profiles with truss-like cores: wavenumber content, forced response and influence of periodicity perturbations. J Sound Vib 2007;304(3–5):691–721.
[6] Chen K, Neugebauer A, Goutierre T, Tang A, Glicksman L, Gibson LJ. Mechanical and thermal performance of aerogel-filled sandwich panels for building insulation. Energy Build 2014;76:336–46.
[7] Sypeck DJ, Wadley HNG. Cellular metal truss core sandwich structures. Adv Eng Mater 2002;4(10):759–64.
[8] Deshpande VS, Fleck NA, Ashby MF. Effective properties of the octet-truss lattice material. J Mech Phys Solids 2001;49(8):1747–69.
[9] Xiong J, Vaziri A, Ma L, Papadopoulos J, Wu L. Compression and impact testing of two-layer composite pyramidal-core sandwich panels. Compos Struct 2012;94(2):793–801.
[10] Queheillalt DT, Wadley HNG. Titanium alloy lattice truss structures. Mater Des 2009;30(6):1966–75.
[11] Kooistra GW, Queheillalt DT, Wadley HNG. Shear behavior of aluminum lattice truss sandwich panel structures. Mater Sci Eng A Struct Mater Properties Microstruct Process 2008;472(1–2):242–50.
[12] Chiras S, Mumm DR, Evans AG, Wicks N, Hutchinson JW, Dharmasena K, et al. The structural performance of near-optimized truss core panels. Int J Solids Struct 2002;39(15):4093–115.
[13] Lee BK, Kang KJ. A parametric study on compressive characteristics of wire-woven bulk Kagome truss cores. Compos Struct 2010;92(2):445–53.
[14] Hyun S, Karlsson AM, Torquato S, Evans AG. Simulated properties of Kagome and tetragonal truss core panels. Int J Solids Struct 2003;40(25):6989–98.
[15] Kang K-J. A wire-woven cellular metal of ultrahigh strength. Acta Mater 2009;57(6):1865–74.
[16] Lee YH, Lee BK, Jeon I, Kang KJ. Wire-woven bulk Kagome truss cores. Acta Mater 2007;55(18):6084–94.
[17] Ullah I, Elambasseril J, Brandt M, Feih S. Performance of bio-inspired Kagome truss core structures under compression and shear loading. Compos Struct 2014;118:294–302.
[18] Wang J, Evans AG, Dharmasena K, Wadley HNG. On the performance of truss panels with Kagome cores. Int J Solids Struct 2003;40(25):6981–8.
[19] Xiong J, Wang B, Ma L, Papadopoulos J, Vaziri A, Wu L. Three-dimensional composite lattice structures fabricated by electrical discharge machining. Exp Mech 2014;54(3):405–12.
[20] Zhang GQ, Wang B, Ma L, Xiong J, Wu LZ. Response of sandwich structures with pyramidal truss cores under the compression and impact loading. Compos Struct 2013;100:451–63.
[21] Che L, Xu G-D, Zeng T, Cheng S, Zhou X-W, Yang S-C. Compressive and shear characteristics of an octahedral stitched sandwich composite. Compos Struct 2014;112:179–87.
[22] Lee BK, Kang KJ. Compressive strength of tube-woven Kagome truss cores. Scr Mater 2009;60(6):391–4.
[23] Queheillalt DT, Wadley HNG. Pyramidal lattice truss structures with hollow trusses. Mater Sci Eng A Struct Mater Properties Microstruct Process 2005;397(1–2):132–7.
[24] Yin S, Wu L, Ma L, Nutt S. Pyramidal lattice sandwich structures with hollow composite trusses. Compos Struct 2011;93(12):3104–11.
[25] Fan HL, Fang DN. Enhancement of mechanical properties of hollow-strut foams: analysis. Mater Des 2009;30(5):1659–66.
[26] Qiao PZ, Fan W, Davalos JF, Zou GP. Optimization of transverse shear moduli for composite honeycomb cores. Compos Struct 2008;85(3):265–74.
[27] Deshpande VS, Fleck NA. Collapse of truss core sandwich beams in 3-point bending. Int J Solids Struct 2001;38(36–37):6275–305.
[28] Hwang J-S, Choi T-G, Lee D, Lyu M-Y, Lee DG, Yang D-Y. Dynamic and static characteristics of polypropylene pyramidal kagome structures. Compos Struct 2015;131:17–24.
[29] Allen HG. Analysis and design of structural sandwich panels. 1st ed. Oxford, New York: Pergamon Press; 1969.
[30] Ashby MF. Metal foams: a design guide. Boston: Butterworth-Heinemann; 2000.